A Numerical Model for Heat and Moisture Transfer in Porous Media of Building Envelopes

Talita Scussiato
Civil Engineering Department
Aeronautics Institute of Technology
Sao Jose dos Campos, Brazil
talita.scussiato@gmail.com

William Hideki Ito
Civil Engineering Department
Aeronautics Institute of Technology
Sao Jose dos Campos, Brazil
ito.william@yahoo.com

Jaqueline Ramis
Civil Engineering Department
Aeronautics Institute of Technology
Sao Jose dos Campos, Brazil
jacramis23@gmail.com

Paulo Ivo Braga de Queiroz
Civil Engineering Department
Aeronautics Institute of Technology
Sao Jose dos Campos, Brazil
pi@ita.br

Received: 1 January 2022 | Revised: 2 February 2022 | Accepted: 3 March 2022

Abstract-This study presents a one-dimensional quantitative analysis of unsaturated flow in natural stones using a numerical model (Finite Difference Method) and a mass balance for the heat flow. For that, we considered heat and moisture transfer between the external environment and a porous media (sandstone and limestone) with homogeneous characteristics. For unsaturated water flow, Richards' equation and the formulation proposed by Gardner for volumetric water content and hydraulic conductivity were considered. The results of the numerical analysis showed that the evaporation of porewater throughout summer days (January 3rd and 4th) considerably reduced the temperature of the roof by about 8°C. The accumulated conductive heat flow and the volumetric water content also had a reduction due to the evaporation process. This fact indicates that evaporation can be useful in providing thermal comfort and, consequently, in improving the energetic efficiency of buildings with natural stones as envelope.

Keywords-Richards' equation; heat transfer; thermal comfort; porous Media

I. INTRODUCTION

Natural stones are used as major components of building envelopes of several historical constructions. The porosity of these natural stones can be greater than those found in other cladding materials, which might influence the decrease of water content absorbed by the capillarity due to evaporation. Some studies have suggested that the moisture transfer between cladding materials and the external environment plays a major role in the thermal comfort inside these buildings [1]. The use of evaporative processes in roofs to enhance thermal comfort in buildings is not an innovation per se, and numerical and experimental modeling of these solutions is frequent in research nowadays. A review of the evaporative method to improve thermal comfort due to the reduction of heat flux through the roof was discussed in [2], whereas authors in [3] presented a review of evaporative cooling systems for buildings. Numerical studies became more frequent in the literature due to the improvement of personal computer processing capacity in recent years. Authors in [4] presented a model based on the Finite Differences Method to evaluate the external surface temperature of a roof using the accumulated internal surface heat flux and the evaporation rate. Authors in [5] carried out a two-dimensional numerical model of evaporation on a plate of the heat exchanger. They showed that ambient temperature, relative humidity, and wind speed have a significant impact on the evaporation and on the reduction of plate temperature. Authors in [6] showed the efficiency of Phase Change Materials (PCM) in the thermal comfort of buildings. Similar results were achieved by other researchers, e.g. in [7-12] among others.

Moisture exchange with the external environment has a great importance to the thermal comfort inside buildings, mainly because the water absorbed by the pores of the rock (or other cladding materials like concrete) migrates to the surface and evaporates. As a result, the absorption of the latent heat cools it [4, 8]. Since the reduction of CO_2 emissions has become a priority to many countries due to the concern of climate change, many studies have focused on improving thermal comfort in building environment with minimal energy consumption. Meantime, there are only a few researches that take in account the influence of the moisture in thermal flow. Following this trend and improving the works already done in this field, the present paper suggests a novel method to evaluate the evaporative process applied to thermal exchanges in a building's roof. To do so, we present a numerical study where we solved the Richard's equation by Finite Difference Method in a one-dimensional model. We compared two types of material envelop in two different days, one humid and other

Corresponding author: Talita Scussiato

dry, and analyzed the influence of external weather conditions in the variation of internal temperature.

II. THEORETICAL FRAMEWORK

Modeling heat and moisture transfer in porous materials is considered a complex task mainly because several phenomena must be evaluated, such as:

- Energy balance
- Solar and nocturnal atmospheric radiation
- Gray body radiation emission by the roof
- Heat conduction in roof slab
- Convective heat transfer between roof and atmosphere
- Heat transfer in evaporative processes
- Water flow in unsaturated porous media.

The following sections briefly describe each of these processes and their equations adopted in this work.

A. Energy Balance

In steady-state conditions, the energy flow balance is written as the sum of the heat flows involved in the thermal exchanges, as indicated in Figure 1 and expressed in (1)

$$q"_I + q" + q"_c - q"_r = q"_e \quad (1)$$

where $q"_I$ is the solar radiation flow, $q"$ is the conductive heat flow, $q"_c$ is the convective heat flow, $q"_r$ is the gray body radiation flow, and $q"_e$ is the evaporative heat flow.

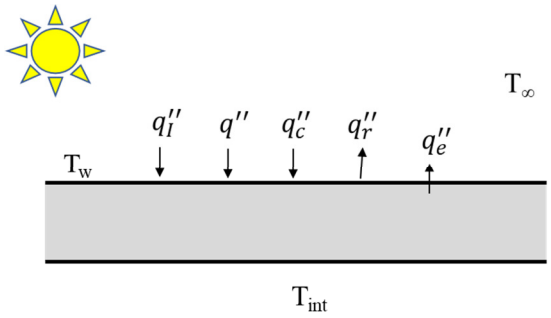

Fig. 1. Heat flow on the roof of a building.

Solar radiation is by far the most important heat source in buildings. For this reason, there are several models available to calculate this parameter [14], which have been used [15] to study the sol-air temperature in a natural stone (marble). Following the work of [13], the authors evaluated the induced stress by daily variation of temperature in external façades using a model developed by [16], which is the model that supported the development of the simplified model by [14] for clear-sky radiation. According to several solar radiation models, a building envelope (wall or roof) absorbs 3 different types of radiation from its surroundings, as shown in (2):

$$q"_I = \alpha_r(I_D \cdot \cos\theta_z + I_d + I_R) \quad (2)$$

where α_r is the shortwave radiation absorbance, I_D is the direct solar radiation attenuated by the atmosphere, θ_z is the zenith angle, I_d is the diffuse sky radiation, and I_R is the solar radiation reflected by surrounding buildings.

Night sky radiation can be considered by (3) [17]:

$$q"_{I,noct} = (1 + KG^2) \cdot 8.78 \times 10^{-13} T_\infty{}^{5.852} RH^{0.07195} \quad (3)$$

where KG is an index that depends on the cloud cover, T_∞ is the air temperature, and RH is the relative humidity.

Radiation energy is transmitted via electromagnetic waves, and it can be represented by gray body radiation. It is defined by the modified Stefan law presented in (4) [18]:

$$q"_r = \sigma\varepsilon T_w^4 \quad (4)$$

where ε is the radiation emissivity, σ is the Stefan-Boltzmann constant (5.67×10^{-8}W/m^{2}K^4), and T_w is the surface temperature of the outer (outdoor) portion of the roof.

Fourier law describes heat conduction in a continuum medium, and it can be represented by (5) and (6):

$$q" = -\frac{l}{R_w}(T_{int} - T_w) \quad (5)$$

where T_{int} is the indoor temperature, R_w is the thermal resistance of the roof, and l is the roof slab thickness.

The hypothesis of steady-state flow assumed in the present work seems reasonable, since a great part of the transient condition (over 90%) is dissipated in less than two hours.

Convective heat transfer between roofs and the external environment can be calculated by two distinct formulations: artificially or naturally induced convection. Both models assess the convective heat transfer by (6):

$$q"_c = h_c(T_\infty - T_w) \quad (6)$$

where h_c is the convective heat transfer coefficient.

Heat transfer by forced convection was estimated through a dimensionless model in [10, 20], where h_c is estimated by (7) for Nusselt number (Nu):

$$Nu = h_c\frac{L_{eq}}{k_a} = 0.036 \cdot Pr^{0.43}(Re^{0.8} - 9200)\left(\frac{\mu_\infty}{\mu_w}\right)^{0.25} \quad (7)$$

where L_{eq} is the equivalent length, k_a is the air thermal conductivity, Pr is the Prandtl number, Re is the Reynolds number, μ_∞ is the absolute air viscosity in the atmosphere, and μ_w is the absolute air viscosity at the roof temperature. The viscosity correction $\left(\frac{\mu_\infty}{\mu_w}\right)^{0.25}$ can be neglected for gases.

The equivalent length refers to the longest building length in the wind direction for a finite length building, expressed by:

$$L_{eq} = min\left[\frac{B}{\sin\theta}, \frac{L}{\cos\theta}\right] \quad (8)$$

where B is the building plan width, L is the building plan length, and θ is the wind direction.

The free convection coefficient is estimated by the model presented in [20, 21]:

$$Nu = c(Gr \cdot Pr)^n \quad (9)$$

$$Sh = c(Gr \cdot Sc)^n \quad (10)$$

where Gr is the Grashof number, Sh is the Sherwood number, and c and n are constants (see Table I).

Grashof number (Gr) is defined by (11) [17]:

$$Gr = \beta g {L_{eq}}^3 \frac{(T_w - T_\infty)}{\nu^2} \quad (11)$$

where g is the gravitational acceleration (9.81m/s^2) and β is the coefficient of the thermal expansion of the air, which is the inverse of the temperature for an ideal gas.

The estimates of the evaporative flux and the heat transfer due to this process are calculated using an iterative process, given that one depends on the other. According to the model presented in [22], the evaporation flow is estimated in a very similar way to the convective flow process, which involves forced or free convection. The evaporative flow is calculated by:

$$F_{ev} = -\left(\frac{Sh \cdot D^v \cdot (\chi_w - \chi_\infty)}{L_{eq}}\right) \quad (12)$$

where F_{ev} is the evaporative mass flux, D_v is the molecular diffusivity of water vapor in the air, and χ_w, χ_∞ are the mass concentration of water vapor at the surface and in the free atmosphere respectively.

In this study, the forced convection uses the dimensionless Sherwood number (Sh) for mass transfer, as presented in (13):

$$Sh = 0.036 Sc^{0.43}(Re^{0.8} - 9200) \quad (13)$$

where Sc is the Schmidt number.

Mass concentration of water vapor (absolute humidity or χ) can be expressed as in:

$$\chi = \frac{M_w \cdot u_v^{air}}{RT} \quad (14)$$

where M_w is the molar mass of water, u_v^{air} is the partial pressure of water vapor, and R is the universal gas constant.

TABLE I. CONSTANTS c AND n FOR FREE CONVECTION ON A HORIZONTAL PLATE AT UNIFORM TEMPERATURE BY [20, 21]

Surface orientation	$Gr.Pr$	c	n	Regime
Hot surface up	10^5 to 2×10^7	0.54	1/4	Laminar
Cold surface down	2×10^7 to 3×10^{10}	0.14	1/3	Turbulent
Hot surface down or cold surface up	3×10^5 to 3×10^{10}	0.27	1/4	Laminar

The partial pressure of water vapor (u_v^{air}) is calculated with the relative humidity (RH) given by:

$$RH = \frac{u_v^{air}}{u_{v0}^{air}} \quad (15)$$

where u_{v0}^{air} is the saturation pressure of water vapor. In the present study, this variable is given by Tetens equation, as shown in [23, 24]:

$$u_{v0}^{air} = 0.61078 \exp\left(\frac{17.27 \cdot T}{T + 237.3}\right) \quad (16)$$

where T is the temperature (°C).

According to [22], the difference of air density above the roof must be considered for simultaneous heat and water vapor transfer analysis. Hence, the concept of virtual temperature is introduced to conveniently express the difference in density between dry and moist air at temperature T. This relationship is represented by:

$$T_v = \frac{T}{\left(1 - (1 - \varepsilon_w)\frac{u_v^{air}}{\bar{u}_a}\right)} \approx T\left(1 + (1 - \varepsilon_w)\frac{u_v^{air}}{\bar{u}_a}\right) \quad (17)$$

where ε_w is the ratio of molecular weights of water vapor and air, taken as 0.622, and $\bar{u}_a$ is the absolute pressure of the air-vapor mixture. Hence, $T_w - T_\infty$, in (11) should be replaced by:

$$T_{vw} - T_{v\infty} \approx (T_w - T_\infty) + \frac{0.38\left(T_w u_{vw}^{air} - T_\infty u_{v\infty}^{air}\right)}{\overline{u_a}} \quad (18)$$

where u_{vw}^{air} and $u_{v\infty}^{air}$ are the partial vapor pressure near the roof and in the atmosphere respectively.

Heat loss/gain due to evaporation/condensation is expressed by:

$$q"_e = h_{vap} \cdot F_{ev} \quad (19)$$

where h_{vap} is the enthalpy of water evaporation.

B. Water Flow in Unsaturated Porous Media

A great number of numerical models considering the unsaturated flow in porous media rely on Richards' equation, which can be represented in a mixed form by [25]:

$$\frac{\partial \theta_w}{\partial t} = \frac{\partial}{\partial z}\left[K(\psi)\frac{\partial(\psi + z)}{\partial z}\right] \quad (20)$$

where θ_w is the volumetric water content, t is the time, K is the hydraulic conductivity and ψ is the water matric suction, that is, the difference between air pressure and pore water pressure.

The unsaturated formulation was proposed by Gardner [35] where the volumetric water content of a porous medium can be estimated as:

$$\theta_w = \theta_r + (\theta_s - \theta_r)e^{\alpha\psi} \quad (21)$$

where θ_r is the residual water content, θ_s is the saturated water content, α is the air entry suction parameter, and ψ is the matric suction.

In the formulation proposed by [35], water hydraulic conductivity (K) is represented by:

$$K = k_s e^{\alpha\psi} \quad (22)$$

where k_s is the saturated hydraulic conductivity.

III. MATERIALS AND METHODS

The input data used in this work are representative of a typical summer day in Brazil. The analysis was conducted using porous rock materials (sandstones and limestones), which are used in several historical buildings. A C++ code was implemented to solve the differential equations.

C. Assumptions Assumed Prior to the Analysis

The following assumptions were considered to simplify the modeling:

- The flow is one-dimensional
- The heat flow is in steady-state condition
- The water flow is in a transient regime
- The airflow is negligible
- The indoor temperature (T_{int}) is constant at 23°C
- The porous media are considered homogeneous
- The thermal conductivity of the porous media is constant concerning the volumetric water content and temperature.

D. Weather Data

In the present study, meteorological data of Ouro Preto – Minas Gerais, Brazil (latitude: 20°23'8", longitude: 43°30'13", altitude: 1.200m above sea level) are considered. The location was chosen because many of the preserved historical buildings in Brazil are located in this area. Meteorological data, including wind velocity (U) and direction (θ), relative humidity (RH), and air temperature (T_∞) were obtained from a weather station at the Federal University of Ouro Preto. The proposed methodology was applied in the interval between January 3rd, 2013 and January 4th, 2013, to evaluate the evaporative-cooling roof effect. The input data used in this paper are presented in Figure 2. On January 3rd, the air temperature varied from 27°C to 17°C, mean wind velocity was about 3.8m/s from 10:00 to 19:00, relative humidity varied from 34% to 100%, and the maximum solar radiation of 870W/m^2 occurred at 11:13. Similar behavior was verified for January 4th, in which the air temperature varied from 25°C to 17°C and the mean wind velocity was about 4m/s, relative humidity varied from 55% to 100%, and the solar radiation was almost coincident with the preceding day. According to these data, we can conclude that January 4th was wetter, colder, and less windy than January 3rd.

E. Heat Flow and Evaporation

Considering an internal environment with constant temperature T_{int}=23°C, a quasi-Newton-Raphson scheme was used to find temperature T_w, as shown in (23):

$$T_{w,i+1} = \frac{\frac{1}{R_w}T_{int} + q''_I + hT_\infty + 3\sigma\varepsilon T_w^4 - h_{vap}F_{ev}}{\frac{1}{R_w} + h + 4\sigma\varepsilon T_w^3} \quad (23)$$

F. Porous Roof Slab

Sandstone and limestone slabs are the unsaturated porous media considered in this study. Both materials were assumed to be homogeneous and without cracks. They were chosen because they are abundant in Southeast Brazil, where Ouro Preto is located. In order to characterize two hypothetical constructions with these materials, some of their properties were taken from the literature (Table II). Both models have a thickness of 0.1m, a building plan width B of 8m, and a building plan length L of 10m. Figure 3 shows the water retention curves of sandstone and limestone used, obtained by the use of van Genuchten parameters [33] described in [32].

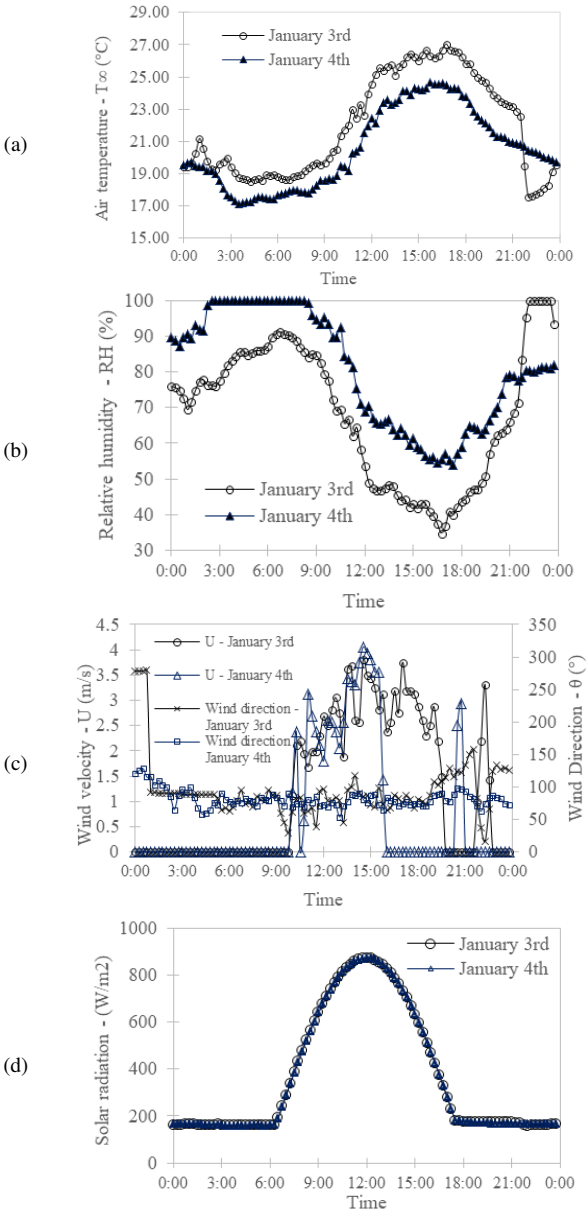

Fig. 2. Environmental conditions for January 3rd and 4th, 2013: (a) Air temperature, (b) relative humidity, (c) wind velocity and direction, (d) solar radiation ($I_D \cdot \cos\theta_z$) where θ_z is the zenith angle.

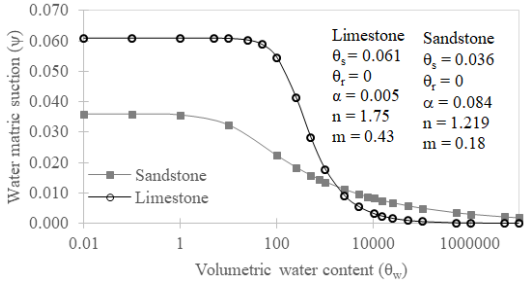

Fig. 3. Water retention curve for limestone and sandstone fitted with the van Genuchten (VG) model.

TABLE II. PROPERTIES OF SANDSTONE AND LIMESTONE USED IN THIS STUDY

Parameter	Sandstone	Limestone	Unit	Ref.
Thermal conductivity (k_r)	1.83	2.5	W/m.K	[26, 27]
Radiation emissivity (ε)	0.935	0.87	-	[28, 29]
Saturated hydraulic conductivity (k_s)	$8x10^{-5}$	$5x10^{-7}$	m/s	[30, 31]*
Saturated water content (θ_s)	0.036	0.061	-	[32]
Residual water content (θ_r)	0	0	-	[32]
Air-entry parameter (α)	0.084	0.005	m^{-1}	[32]
Porosity (n_p)	3.4	1.75	%	[32]
Bulk density (ρ_b)	2.35	2.3	g/cm^3	[32]
*mean value				

G. Unsaturated Flow

The calculation of unsaturated flow was based on the work developed by Mannich [34]:

$$\theta_w = \theta_r + (\theta_s - \theta_r)e^{\alpha\psi}, K = k_s e^{\alpha\psi}$$

Mannich uses a finite volume in spatial discretization and a Crank-Nicholson scheme in time. In this scheme, the equations system is solved simultaneously and the Richards' equation (20) can be rewritten as (24):

$$C(\psi)\frac{\partial\psi}{\partial t} = \frac{\partial q}{\partial z} \quad (24)$$

where q and $C(\psi)$ can be defined as:

$$q = K(\psi)\frac{\partial\psi}{\partial z} + K(\psi)\,,\ C(\psi) = \frac{\partial\theta}{\partial\psi} \quad (25)$$

The equation for internal nodes, representing the capillary potential calculated at the end of the time interval, can be expressed as:

$$P_i\psi_i^{j+1} = W_i\psi_{i-1}^{j+1} + E_i\psi_{i+1}^{j+1} + B_i \quad (26)$$

where ψ_i^j is the matric suction in grid node i at time j.

The coefficients of (26) are expressed as:

$$W_i = \frac{k_{i-\frac{1}{2}}^{j+1}}{\Delta z^2}, E_i = \frac{k_{i+\frac{1}{2}}^{j+1}}{\Delta z^2}, P_i = \frac{C_i^{j+\frac{1}{2}}}{\Delta t} + W_i + E_i \quad (27)$$

$$B_i = \frac{C_i^{j+\frac{1}{2}}\psi_i^j}{\Delta t} + \frac{1}{\Delta z}\left[k_{i+\frac{1}{2}}^j\left(\frac{\psi_{i+1}^j - \psi_i^j}{\Delta z} + 1\right) - k_{i-\frac{1}{2}}^j\left(\frac{\psi_i^j - \psi_{i-1}^j}{\Delta z} + 1\right) + k_{i+\frac{1}{2}}^{j+1} + k_{i-\frac{1}{2}}^{j+1}\right] \quad (28)$$

Half indexes like in $k_{i-\frac{1}{2}}^{j+1}$ denote that the hydraulic conductivity is calculated with the average suction between ψ_{i-1}^{j+1} and ψ_i^{j+1}. Hence, $C_i^{j+\frac{1}{2}}$ is the derivative $C = \frac{\partial\theta_w}{\partial\psi}$ calculated with the average suction $\psi = \frac{\psi_i^{j+1} + \psi_i^j}{2}$.

The bottom of the slab was taken as a moist environment, where $\psi_0 = B_0 = 0,\ W_0 = 0,\ E_0 = 0$, and $P_0 = 0$.

For the top of the slab, evaporative mass flux (F_{ev}) was imposed, which means that the coefficients of (26) become $W_n = 1,\ E_n = 0,\ P_n = 1$, and $B_n = \left(\frac{q^j - k^j_{n-\frac{1}{2}}}{k^j_{n-\frac{1}{2}}}\right)\Delta z$.

The coefficient q^j is represented by:

$$q^j = F_{ev} \quad (29)$$

For the finite element difference grid, the time interval (Δt) considered was of 15 minutes over the course of a day, and the space interval (Δz) was 0.01m for a total thickness L=0.1m for sandstone roof slab. The main goal of the proposed methodology is the consideration of the evaporative processes through the coefficients of water flow in the heat flux.

IV. RESULTS AND DISCUSSION

A. Roof Temperature

Figures 4 and 5 show, respectively, the results of the temperatures calculated for January 3rd and 4th in sandstone and limestone hypothetical roofs. The external air temperatures are also plotted. Two different conditions were considered: with and without evaporation. From 12:00 AM to 6:00 AM, the external air temperature was about 20°C, but the theoretical temperature on the external surface of the roof was about 13°C for sandstone and 15°C for limestone. These almost constant temperatures are explained by the absence of direct solar irradiation. However, from 6:00 AM to 4:00 PM, the temperature of the roof rises until it reaches a peak, and then it falls. During a great part of this interval, the temperature calculated for the external surface of the roof is higher than the external air temperature for both conditions (with and without considering evaporation). Temperature differences occur due to the solar radiation effect, which starts to increase at 6:00 AM and reaches its peak around 12:00 PM (coinciding with maximum roof temperature). After that, the solar radiation continuously decreases until it becomes negligible. From 4:00 PM on, the roof temperature is lower than the temperature of the air for both hypotheses (with and without evaporation).

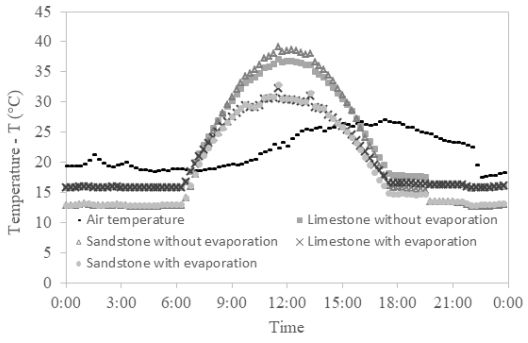

Fig. 4. Temperature of the roof and air on a sunny day (January 3rd).

These results show that the theoretical temperature is almost the same for both materials if the evaporation effect is considered. Without this effect, the difference in temperature reaches 2°C. This can be explained by solar radiation, which was the major phenomenon involved in the calculation. The value of shortwave radiation absorbance (α) used was the same for both materials. The reduction of temperature due to evaporation on January 3rd and 4th (Figures 4 and 5), was about 8°C-7°C for sandstone and 6°C-5°C for limestone. In Figure 4, the outliers observed at 11:30 AM and at 01:15 PM can be explained by the changes in wind direction.

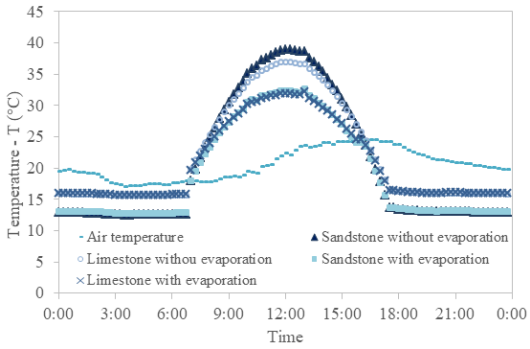

Fig. 5. Temperature in the roof and air on a mild and humid summer day (January 4th).

B. Heat Transfer

Figure 6 presents the conductive heat flow calculated for the examples described above. One can notice that the accumulated conductive heat flow is positive until 9:00 am. Afterward, a reduction in accumulated heat flow from 9:00 AM to 15:00 PM on January 4th is noticeable. Then, it asymptotically stabilizes near -0.4 and -0.2 for conditions neglecting and considering the evaporation effect respectively. This phenomenon occurred due to the absence of wind during this period. Without wind, the roof's temperature does not change, and the system does not exchange heat.

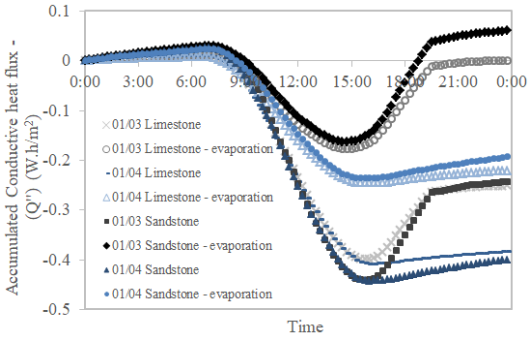

Fig. 6. Accumulated conductive heat flow in sandstone and limestone roofs on two different summer days (January 3rd and 4th).

On January 3rd, the decrease in accumulated heat flux occurred until 03:00 PM. It reached a minimum, and then increased until 06:00 PM, and stabilized in –0.25 for both materials. This happened in a condition without evaporation, and 0 for limestone and 0.05 for sandstone when the evaporation process was taken into consideration. This occurred because the system only reaches stability when wind velocity is zero. The cumulative conductive heat flow is lower for processes that consider the evaporative effect than for those which do not, mainly because the roof loses a lesser amount of energy to the environment due to the lower gradient of temperature between the surfaces. Similarly, if evaporation is not considered, the heat flow is higher because the temperature of the external surface of the roof is also higher. Therefore, it is possible to conclude that the evaporation process causes the reduction of temperature, that is, it consumes heat.

C. Water Flow

Figure 7 shows the cumulated evaporative rate through roof thickness throughout the day. We can see that the maximum evaporation rate is close to 4.5L/m^2 for sandstone on a summer day in Ouro Preto (January 3rd). The minimum evaporative rate of 2.5L/m^2 was verified for limestone on January 4th. One can notice that the cumulated evaporative rate was smaller on January 4th than on January 3rd in both materials. The difference occurred due to the difference in the temperature verified in these two days, which was 2°C lower on January 3rd. The relative humidity was 20% higher and there was less wind throughout the day. It can be pointed out that, for January 4th, the accumulated evaporative rate was smaller than on January 3rd for both materials, because on the 4th the temperature was 2°C lower, the relative humidity 20% higher, and there was less wind during that day.

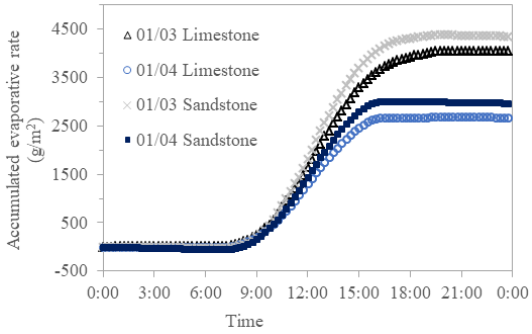

Fig. 7. The accumulated evaporative rate in sandstone and limestone roofs on January 3rd and 4th.

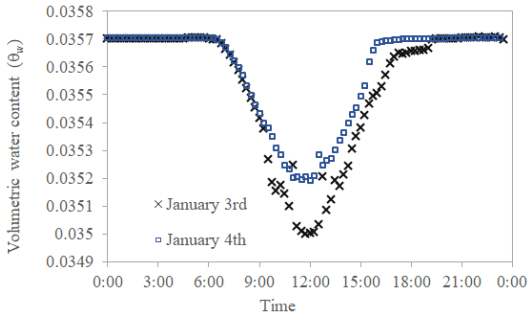

Fig. 8. Volumetric water content (θ_w) on January 3rd in sandstone roof.

Figures 8 and 9 show the volumetric water content for sandstone and limestone roofs on January 3rd and 4th respectively. It is noticeable that the volumetric water content

did not reduce significantly due to the evaporation on sandstone (about 2%). On the other hand, for the limestone roof model, the reduction was of about 15% on January 3rd around 12:00 pm.

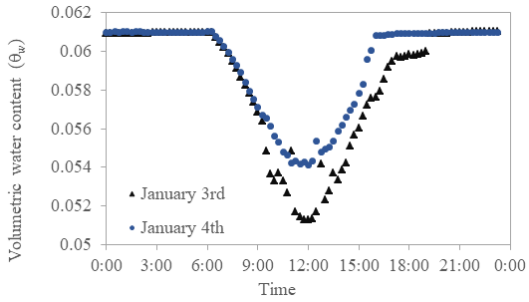

Fig. 9. Volumetric water content (θ_w) on January 4th in limestone roof.

D. Discussion

The current study uses weather data and properties of facade materials to calculate roof temperature. Its main purpose is to model how evaporative roofs improve thermal comfort in buildings. Following the world trend of NZEB (Net Zero Energy Buildings) [35], this study shows that the internal environment temperature may be reduced by the evaporative process. The choice of appropriate envelope material can reduce the use of air-conditioning. The main contribution presented here is the method of accounting for the evaporative process in the boundary condition of water flow in a finite volume scheme for unsaturated materials. Similar works [1, 34] do not consider the coupled effects of water flow and evaporation associated to heat flow.

V. CONCLUSION

This study presented a numerical calculation, in one-dimensional Finite Difference Method, for unsaturated flow using Richards' equation and Gardner's formulation for volumetric water content and saturated hydraulic conductivity. For the heat flow, the balance of 5 heat fluxes (solar radiation, conductive, convective, gray body radiation, and evaporative) were considered. The heat and moisture transfer model was carried out for 2 different natural stones (sandstone and limestone) in a hypothetical building located at a historical city in Brazil (Ouro Preto-MG) and under two conditions: with and without evaporation.

This study showed that, for both materials, the evaporation process of the porewater throughout the day considerably reduces the temperature of the roof. Around 12:00 pm, the roof temperature dropped approximately by 8.5°C on January 3 and 7.5°C on January 4 due to the evaporation of the water contained within the pores of the sandstone roof. The temperature was 2°C higher on sandstone roofs when compared to limestone roofs. On January 3, during an entire summer day, we observed a maximum accumulated evaporation rate of about 4.5L/m^2 of sandstone roof area. Moreover, the maximum reduction of water content for the limestone roof was about 15%, around 12:00 pm.

The numerical analysis results show that the evaporation of porewater throughout summer days considerably reduces the temperature of the roof and the accumulated conductive heat flow. The results indicate that evaporative processes can be useful in order to provide hygrothermal comfort with energetic efficiency for buildings having sandstone or limestone as envelope material for the summer day design conditions.

ACKNOWLEDGEMENT

The authors are grateful to Maria Luiza Teófilo Gandini and Gilberto Queiroz da Silva for providing the data of the weather station of Ouro Preto Federal University.

REFERENCES

[1] L. Zhang, R. Zhang, Y. Zhang, T. Hong, Q. Meng, and Y. Feng, *The Impact of Evaporation Process on Thermal Performance of Roofs Model Development and Numerical Analysis*. Berkeley, CA, USA: Lawrence Berkeley National Laboratory, 2016.

[2] G. N. Tiwari, A. Kumar, and M. S. Sodha, "A review—Cooling by water evaporation over roof," *Energy Conversion and Management*, vol. 22, no. 2, pp. 143–153, Jan. 1982, https://doi.org/10.1016/0196-8904(82)90036-X.

[3] P. M. Cuce and S. Riffat, "A state of the art review of evaporative cooling systems for building applications," *Renewable and Sustainable Energy Reviews*, vol. 54, pp. 1240–1249, Feb. 2016, https://doi.org/10.1016/j.rser.2015.10.066.

[4] L. Zhang, X. Liu, Q. Meng, and Y. Zhang, "Experimental study on the impact of mass moisture content on the evaporative cooling effect of porous face brick," *Energy Efficiency*, vol. 9, no. 2, pp. 511–523, Apr. 2016, https://doi.org/10.1007/s12053-015-9377-8.

[5] N. Grich, W. Foudhil, S. Harmand, and S. B. Jabrallah, "Numerical simulation of water spray transport along a plate of a heat exchanger," *Journal of Thermal Analysis and Calorimetry*, vol. 143, no. 5, pp. 3887–3895, Mar. 2021, https://doi.org/10.1007/s10973-020-09356-w.

[6] N. B. Khedher, "Numerical Study of the Thermal Behavior of a Composite Phase Change Material (PCM) Room," *Engineering, Technology & Applied Science Research*, vol. 8, no. 2, pp. 2663–2667, Apr. 2018, https://doi.org/10.48084/etasr.1824.

[7] S. Ahmadi, M. Irandoost Shahrestani, S. Sayadian, M. Maerefat, and A. Haghighi Poshtiri, "Performance analysis of an integrated cooling system consisted of earth-to-air heat exchanger (EAHE) and water spray channel," *Journal of Thermal Analysis and Calorimetry*, vol. 143, no. 1, pp. 473–483, Jan. 2021, https://doi.org/10.1007/s10973-020-09268-9.

[8] J. I. Kindangen and M. K. Umboh, "Design of evaporative-cooling roof for decreasing air temperatures in buildings in the humid tropics," *AIP Conference Proceedings*, vol. 1818, no. 1, Mar. 2017, Art. no. 020023, https://doi.org/10.1063/1.4976887.

[9] T. Chati, K. Rahmani, T. T. Naas, and A. Rouibah, "Moist Air Flow Analysis in an Open Enclosure. Part A: Parametric Study," *Engineering, Technology & Applied Science Research*, vol. 11, no. 5, pp. 7571–7577, Oct. 2021, https://doi.org/10.48084/etasr.4344.

[10] P. Tewari, S. Mathur, and J. Mathur, "Thermal performance prediction of office buildings using direct evaporative cooling systems in the composite climate of India," *Building and Environment*, vol. 157, pp. 64–78, Jun. 2019, https://doi.org/10.1016/j.buildenv.2019.04.044.

[11] E. Zanchini and C. Naldi, "Energy saving obtainable by applying a commercially available M-cycle evaporative cooling system to the air conditioning of an office building in North Italy," *Energy*, vol. 179, pp. 975–988, Jul. 2019, https://doi.org/10.1016/j.energy.2019.05.065.

[12] W. Aich, "3D Buoyancy Induced Heat Transfer in Triangular Solar Collector Having a Corrugated Bottom Wall," *Engineering, Technology & Applied Science Research*, vol. 8, no. 2, pp. 2651–2655, Apr. 2018, https://doi.org/10.48084/etasr.1857.

[13] J. E. Ramis, "Modelagem da transferência de calor em lajes de cobertura de terminais de passageiros aeroportuários," Ph.D. dissertation, Instituto Tecnológico de Aeronáutica, São José dos Campos, Brasil, 2016.

[14] *ASHRAE, Fundamentals: 2001 Ashrae Handbook, Inch-Pound Edition. New York, NY, USA: American Society of Heating, Refrigerating and Air-Conditioning Engineers, 2001.*

[15] W. H. Ito *et al.*, "On the Thermal Stresses Due to Weathering in Natural Stones," *Applied Sciences*, vol. 11, no. 3, Jan. 2021, Art. no. 1188, https://doi.org/10.3390/app11031188.

[16] M. Iqbal, *An Introduction To Solar Radiation*. New York, NY, USA: Academic Press, 1983.

[17] M. A. Goforth, G. W. Gilchrist, and J. D. Sirianni, "Cloud effects on thermal downwelling sky radiance," in *Proceedings of SPIE*, Orlando, FL, USA, Apr. 2002, vol. 4710, pp. 203–213, https://doi.org/10.1117/12.459570.

[18] T. L. Bergman, F. P. Incropera, D. P. DeWitt, and A. S. Lavine, *Fundamentals of Heat and Mass Transfer*, 7th edition. Hoboken, NJ, USA: John Wiley & Sons, 2011.

[19] S. Whitaker, *Elementary Heat Transfer Analysis*. New York, NY, USA: Pergamon, 1976.

[20] M. N. Ozisik, *Heat Transfer: A Basic Approach*, International Ed edition. New York, NY, USA: McGraw-Hill, 1985.

[21] W. H. McAdams, *Heat transmission*, 3rd edition. New York, NY, USA: McGraw-Hill, 1954.

[22] J. Monteith and M. Unsworth, *Principles of Environmental Physics: Plants, Animals, and the Atmosphere*, 4th edition. Amsterdam, Boston: Academic Press, 2013.

[23] O. Tetens, "Uber einige meteorologische Begriffe," *Zeitschrift Geophysic*, vol. 6, pp. 297–309, 1930.

[24] F. W. Murray, "On the Computation of Saturation Vapor Pressure," *Journal of Applied Meteorology and Climatology*, vol. 6, no. 1, pp. 203–204, Feb. 1967, https://doi.org/10.1175/1520-0450(1967)006<0203:OTCOSV>2.0.CO;2.

[25] L. A. Richards, "Capillary conduction of liquids through porous mediums," *Physics*, vol. 1, no. 5, pp. 318–333, Nov. 1931, https://doi.org/10.1063/1.1745010.

[26] M. N. Ozisik, *Heat Conduction*, 2nd ed. New York, NY, USA: Wiley, 1993.

[27] J. Thomas, R. R. Frost, and R. D. Harvey, "Thermal conductivity of carbonate rocks," *Engineering Geology*, vol. 7, no. 1, pp. 3–12, Jun. 1973, https://doi.org/10.1016/0013-7952(73)90003-3.

[28] C. D. Kern, *Evaluation of Infrared Emmission of Clouds and Ground as Measured by Weather Satellites*. Office of Aerospace Research, US Air Force, 1965.

[29] E. Barreira, E. Bauer, N. Mustelier, and V. Freitas, "Measurement of materials emissivity – Influence of the procedure," in *13th International Workshop on Advanced Infrared Technology & Applications*, Pisa, Italy, Sep. 2015.

[30] M. Farzamian, F. A. Monteiro Santos, and M. A. Khalil, "Estimation of unsaturated hydraulic parameters in sandstone using electrical resistivity tomography under a water injection test," *Journal of Applied Geophysics*, vol. 121, pp. 71–83, Oct. 2015, https://doi.org/10.1016/j.jappgeo.2015.07.014.

[31] P. A. Domenico and F. W. Schwartz, *Physical and chemical hydrogeology*. New York, NY, USA: Wiley, 1990.

[32] K. Parajuli, M. Sadeghi, and S. B. Jones, "A binary mixing model for characterizing stony-soil water retention," *Agricultural and Forest Meteorology*, vol. 244–245, pp. 1–8, Oct. 2017, https://doi.org/10.1016/j.agrformet.2017.05.013.

[33] M. Th. van Genuchten, "A Closed-form Equation for Predicting the Hydraulic Conductivity of Unsaturated Soils," *Soil Science Society of America Journal*, vol. 44, no. 5, pp. 892–898, 1980, https://doi.org/10.2136/sssaj1980.03615995004400050002x.

[34] M. Mannich, "Desenvolvimento de Solucoes Analiticas e Numericas da Equacao de Richards," Ph.D. dissertation, Universidade Federal do Parana, Curitiba, Brazil, 2008.

[35] W. R. Gardner, "Some Steady-State Solutions of the Unsaturated Moisture Flow Equation with Application to Evaporation from a Water Table," *Soil Science*, vol. 85, pp. 228–232, Apr. 1958, https://doi.org/10.1097/00010694-195804000-00006.